New Journal of Physics
The open-access journal for physics

Electronic properties of $LaO_{1-x}F_xFeAs$ in the normal state probed by NMR/NQR

H-J Grafe[1,7], G Lang[1], F Hammerath[1], D Paar[1,2], K Manthey[1], K Koch[3], H Rosner[3], N J Curro[4], G Behr[1], J Werner[1], N Leps[1], R Klingeler[1], H-H Klauss[5], F J Litterst[6] and B Büchner[1]

[1] IFW Dresden, Institute for Solid State Research, PO Box 270116, D-01171 Dresden, Germany
[2] Department of Physics, Faculty of Science, University of Zagreb, PO Box 331, HR-10002 Zagreb, Croatia
[3] Max Planck Institute for Chemical Physics of Solids, Nöthnitzer Strasse 40, D-01187 Dresden, Germany
[4] Department of Physics, University of California, Davis, CA 95616, USA
[5] Institut für Festkörperphysik, TU Dresden, D-01069 Dresden, Germany
[6] Institut für Physik der Kondensierten Materie, TU Braunschweig, D-38106 Braunschweig, Germany
E-mail: h.grafe@ifw-dresden.de

New Journal of Physics **11** (2009) 035002 (14pp)
Received 26 November 2008
Published 20 March 2009
Online at http://www.njp.org/
doi:10.1088/1367-2630/11/3/035002

Abstract. We report ^{139}La, ^{57}Fe and ^{75}As nuclear magnetic resonance (NMR) and nuclear quadrupole resonance (NQR) measurements on powders of the new $LaO_{1-x}F_xFeAs$ superconductor for $x = 0$ and 0.1 at temperatures up to 480 K, and compare our measured NQR spectra with local density approximation (LDA) calculations. For all three nuclei in the $x = 0.1$ material, it is found that the local Knight shift increases monotonically with an increase in temperature, and scales with the macroscopic susceptibility, suggesting a single magnetic degree of freedom. Surprisingly, the spin lattice relaxation rates for all nuclei also scale with one another, despite the fact that the form factors for each site sample different regions of $\boldsymbol{q}$-space. This result suggests a lack of any $\boldsymbol{q}$-space structure in the dynamical spin susceptibility that might be expected in the presence of antiferromagnetic correlations. Rather, our results are more compatible with simple quasi-particle scattering. Furthermore, we find that the

[7] Author to whom any correspondence should be addressed.

increase in the electric field gradient at the As cannot be accounted for by LDA calculations, suggesting that structural changes, in particular the position of the As in the unit cell, dominate the NQR response.

Contents

1. Introduction

The recent discovery [1] of superconductivity in the layered ferropnictides $RO_{1-x}F_xFeAs$ (where R is a rare earth element) has raised great interest within the solid state community. Not only does the transition temperature, T_c, reach a maximum at 55 K, but it is strongly dependent on the rare-earth ion and the pressure [2]–[4]. Furthermore, the normal state properties exhibit some unusual features, which are reminiscent of the copper oxide high-temperature superconductors (HTSC). In particular, there is a pseudogap-like decrease of the magnetic susceptibility at low temperatures [5]–[8], and three-dimensional (3D) antiferromagnetic order in the parent (undoped) compound LaOFeAs with $T_N \sim 140$ K. An important difference, however, is that the ferropnictides exhibit metallic properties, and clearly are not Mott insulators [9, 10]. Upon doping, the antiferromagnetic order is destroyed in both families, and a superconducting ground state emerges in the phase diagram. The proximity of superconductivity to an antiferromagnetic ground state and the appearance of the pseudogap features hint at the presence of magnetic correlations in these materials, as in high T_c-cuprates, that may play a critical role in the underlying physics of the superconductivity.

In this paper, we report nuclear magnetic resonance (NMR), and nuclear quadrupole resonance (NQR) investigations of the normal state of $LaO_{0.9}F_{0.1}FeAs$ and LaOFeAs. Our results shed light on the role and importance of magnetic correlations in these compounds. In particular, we find no evidence for strong magnetic correlations in superconducting $LaO_{0.9}F_{0.1}FeAs$. NMR and NQR are well suited to probe magnetic correlations, since they are sensitive local probe techniques giving access to the intrinsic susceptibility, with a nucleus-dependent sensitivity to certain regions in $\boldsymbol{q}$-space. In section 2, we outline the experimental details of sample preparation and characterization, as well as NMR- and theory-related details.

The NMR results on the electronic spin susceptibility are then presented and discussed in section 3. Our Knight shift and spin lattice relaxation rate measurements of three different nuclei (^{75}As, ^{57}Fe and ^{139}La) scale with one another as a function of temperature. This result is surprising, as it suggests that all nuclei couple to the same spin degree of freedom, and that there is little or no $\boldsymbol{q}$-space structure in the dynamical spin susceptibility. If spin fluctuations were present, with a correlation length greater than about one lattice spacing, then the ^{75}As and ^{139}La spin lattice relaxation rates would differ from that of the ^{57}Fe, in contrast with our observations. We also measure the Knight shift of the ^{75}As up to 480 K, in order to investigate the behavior of the spin susceptibility at high temperatures. We find that the shift increases monotonically up to 480 K, showing no sign of a peak as observed in pseudogap studies of the cuprates [11]. Finally, in section 4, we present density functional calculations of the spatial charge distribution and electric field gradient (EFG) at the ^{75}As site in $LaO_{0.9}F_{0.1}FeAs$ and LaOFeAs and compare them with our experimental observations.

2. Experimental details and theoretical methods

2.1. Sample preparation and characterization

Polycrystalline samples of $LaO_{1-x}F_xFeAs$ with $x = 0.1$ and 0 were prepared by standard methods and characterized by x-ray diffraction, resistivity and susceptibility measurements as described in [6, 12]. A value of $T_c \approx 26.0$ K was extracted from these measurements for a fluorine doping of $x = 0.1$. A similar but ^{57}Fe-enriched sample showed a reduced $T_c \approx 20$ K from low-field superconducting quantum interference device (SQUID) measurements, with a reduced Meissner effect. The origin of the reduced T_c is not yet clear. A change in the doping level could be excluded, as the ^{75}As NQR spectrum was unchanged. The undoped (non-superconducting) sample exhibits a structural phase transition from tetragonal to orthorhombic at $T_S \approx 156$ K followed by a spin density wave transition at $T_N \approx 138$ K [13]. For the NMR experiments, an oriented powder of the (unenriched) $x = 0.1$ sample was formed by grinding the material to a powder, mixing with Stycast 1266 epoxy and curing in an external field of 9.2 T.

2.2. NMR and NQR

NMR is a powerful probe of the behavior of the electronic system in the ferropnictides because the nuclei interact with the electrons via quadrupolar and hyperfine interactions. The nuclear Hamiltonian is given by

$$\mathcal{H} = -\gamma_n \hbar I (1+K) H_0 + \frac{h\nu_Q}{2}\left[I_z^2 - \frac{I(I+1)}{3} + \frac{\eta}{6}(I_+^2 + I_-^2)\right], \quad (1)$$

where γ_n and I are the gyromagnetic ratio and the spin of the nucleus, $\hbar$ is Planck's constant, H_0 the applied magnetic field, K is the NMR shift and ν_Q and η are the quadrupole frequency and the asymmetry of the electric field gradient tensor. The quadrupole moment, Q, of nuclei with spin $I > 1/2$ (La, As) interacts with the EFG, which depends on the local charge symmetry. The quadrupolar interaction lifts the degeneracy of the I multiplet, giving rise to $2I + 1$ resonances in an applied field (NMR), and $I - 1/2$ resonances in zero field (NQR).

Table 1. NMR/NQR properties of the studied nuclei. The relative sensitivity for iron assumes 100% ^{57}Fe enrichment.

	I	γ_n (MHz/T)	Q (10^{-28} m^2)	Natural abundance (%)	Relative sensitivity ($^1H = 1$)
^{139}La	7/2	6.014	0.2	≈100	5.9×10^{-2}
^{57}Fe	1/2	1.3757	0	≈2.2	3.4×10^{-5}
^{75}As	3/2	7.2917	0.314	100	2.5×10^{-2}

The Knight shift K arises from the hyperfine interaction between the spins of the electrons and the spins of the nuclei. In the presence of an applied field (NMR), the static field of the polarized electrons creates an additional field at the nuclear sites, yielding a shift, K, of the resonance line with respect to the unshifted Larmor frequency. Furthermore, any time dependence of this hyperfine field (due to electronic spin and orbital moment fluctuations) gives rise to spin lattice relaxation. In general, K can be written as the sum of a temperature-dependent spin part, K_s, and a usually temperature-independent orbital part, K_{orb}. K_s is proportional to the static susceptibility of the electrons at the Fermi level, $\chi_s(q = 0)$:

$$K_s = A_{hf} \cdot \chi_s(q = 0), \tag{2}$$

where A_{hf} is the hyperfine coupling, which depends on the nucleus through the availability of various coupling paths, i.e. on-site coupling or transferred coupling to neighboring atoms.

All of the nuclei are NMR-active in $LaO_{0.9}F_{0.1}FeAs$; we have chosen to focus on ^{139}La, ^{75}As and ^{57}Fe, whose properties are given in table 1. Since La is located out of the FeAs plane, it is expected to be coupled only weakly to the electronic spin system. The EFG at the La site is particularly small, rendering NQR experiments difficult to carry out. On the other hand, As is located directly in the FeAs planes, and therefore should have a comparatively higher coupling to the electronic spins. Moreover, the combination of a large quadrupole moment and EFG allows for direct NQR experiments on the ^{75}As. The spin-1/2 nature of the ^{57}Fe is ideal for contrasting with the ^{75}As in order to distinguish quadrupolar from magnetic effects. However, the low natural abundance of the ^{57}Fe isotope makes it necessary to enrich the sample, using ^{57}Fe during the synthesis. Nevertheless, the sensitivity remains low when compared to the other nuclei, making these experiments more difficult.

When doing NMR on a powder sample, the crystallites are randomly oriented with respect to the applied magnetic field. This implies the random orientation of the magnetic and quadrupolar electric hyperfine tensors, giving rise to broad spectra and reduced signal intensities. Although EFG and magnetic shift tensors can be extracted from powder patterns in principle, we have chosen to exploit the anisotropic character of the magnetic susceptibility of these materials. By letting a mixture of powder and liquid epoxy cure while subjected to an external field, one obtains a powder with its crystallites oriented along the direction of highest susceptibility. In the case of $LaO_{0.9}F_{0.1}FeAs$, the susceptibility is larger in the ab plane, i.e. along two directions. Therefore, we obtain ab oriented samples where the ab planes are parallel to the applied field, with a distribution of the resonance simpler (2D powder) than in the standard powder case.

2.3. LDA calculations

The band structure calculations were performed using the full-potential local-orbital minimum basis code FPLO (version 5.00-19) [14] within the local density approximation (LDA). In the scalar relativistic calculations, the exchange and correlation potential of Perdew and Wang [15] was employed. As basis set La (5s5p/6s6p5d+4f7s7p), Fe (3s3p/4s4p3d+4d5s5p), As (4s4p3d+4d5s5p) and O (2s2p3d+3s3p) were chosen for semicore/valence+polarization states. The high lying states improve the basis, which is especially important for the calculation of the EFG tensor with the components $V_{ij} = \partial V/\partial x_i \partial x_j$. The lower lying states were treated fully relativistic as core states. A well-converged k-mesh of 275 k-points was used in the irreducible part of the Brillouin zone. LaFeAsO was calculated in space group 129 (P4/nmm) with the structural parameters as given in [9]. In order to investigate the influence of F substitution on the O site, the virtual crystal approximation (VCA) was applied and cross-checked with the calculation of super cells[8].

3. Spin susceptibility

In this section, we present results pertaining to the electronic spin susceptibility of the FeAs layers, as probed by ^{139}La, ^{75}As and ^{57}Fe nuclei. Through spectra and relaxation measurements, we probe the temperature dependence of the static and dynamic susceptibility.

3.1. Uniform susceptibility

3.1.1. Knight shift tensor at the ^{57}Fe. Accessing the temperature dependence of the susceptibility at $\boldsymbol{q} = 0$ was done through measurements of the NMR shift for the three studied nuclei, as derived from fitting of experimental spectra. A representative example is given in figure 1, which shows ^{57}Fe NMR data for an unaligned doped $LaO_{0.9}F_{0.1}FeAs$ powder. The data were obtained using the standard spin echo sequence with $\tau = 24\,\mu$s, while sweeping the field at a constant frequency of 12.7 MHz. These spectra correspond to the iron $(1/2 \leftrightarrow -1/2)$ transition at several temperatures. For $T = 20$ K ($T_c < 20$ K at $H_0 = 9.2$ T, see section 2), we can clearly resolve a high-field tail in the spectrum. Since ^{57}Fe has $I = 1/2$, there are no quadrupolar contributions to this spectrum, and in fact this shape is typical of a powder distribution with an anisotropic Knight shift tensor. This interpretation is confirmed by a simulation of such a distribution (see [16, 17]), shown as a solid line in figure 1, allowing us to extract the eigenvalues $K_{1/2/3}$ of the magnetic hyperfine tensor. We find $K_1 = K_2 = 1.35(1)\%$ and $K_3 = 0.85(2)\%$, with the higher uncertainty on K_3 due to the lack of definition of the end of the high-field tail ($K_{1/2}$ relates to the low-field peak). In light of the layered structure, it is reasonable to assume that the principal axes of the magnetic hyperfine tensor lie along the c-axis and within the ab plane, with equal in-plane eigenvalues, and we assign $K_{1/2}$ and K_3 as K_{ab} and K_c. On increasing the temperature, we observe similar spectra, at least for the low-field peak (the poor sensitivity precludes comparison at higher fields). The full lines show again powder simulations, with K_c held at its value at $T = 20$ K so that the high-field decrease remains the same. The low-field peak, which is solely determined by K_{ab}, shows a weak temperature dependence (see figure 2).

[8] In order to come close to the experimental F concentration of 10%, a 4-fold super cell (doubled along a and b), with eight formula units, was calculated. Therefore the space group Pmm2 (#25) was chosen. Replacing one O by F yields the composition of $LaFeAsO_{0.875}F_{0.125}$.

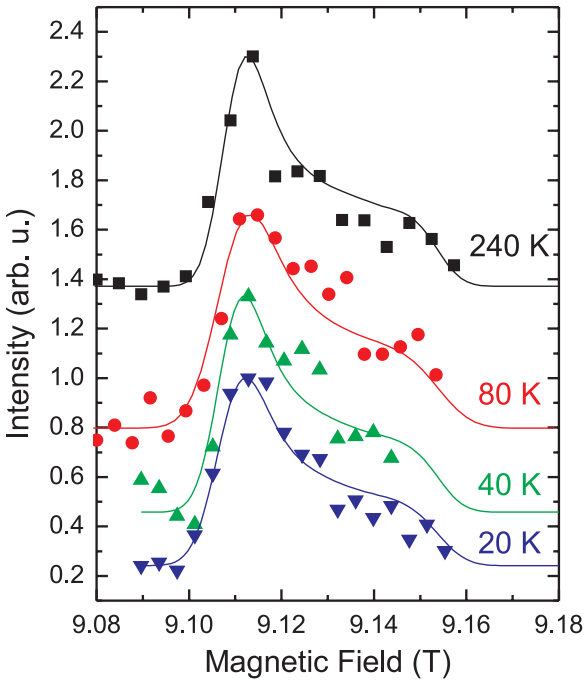

Figure 1. Field sweeped NMR spectra of the ^{57}Fe for different temperatures measured at an applied frequency of 12.7 MHz. The full lines are simulations as described in the text.

If we assign the temperature-independent component to the orbital shift (as is customarily done), we find quite a small (less than 0.1%) spin component of the NMR shift along ab, with most of the shift being of orbital origin ($K^{ab}_{\rm orb} \approx 1.4\%$). Note, however, the much smaller value of K_c compared with K_{ab}. In a similar ^{57}Fe study on $LaFeAsO_{0.7}$, Terasaki *et al* [18] measured an even bigger anisotropy at $T = 30$ K, with a shift of roughly 0.5% along c compared with again 1.4% in the plane. One possibility would be that this strong difference between the c and ab directions originates from a large difference in spin shift, well exceeding an order of magnitude, with an isotropic orbital shift. This would imply a very large anisotropy of the iron hyperfine coupling, since SQUID measurements rule out any such large anisotropy of the susceptibility. Having an isotropic orbital shift in spite of the doping would also likely imply minimum significant mixing of the 3d orbitals. While we cannot rule out that scenario, a more straightforward explanation would be that there is a large orbital shift anisotropy (implying $K^{c}_{\rm orb} \approx 0.8\%$), reflecting the fact that the iron valence shell is not closed. This may yield indications on the average valence of the iron and thus on the doping, as was suggested by Mukhamedshin *et al* [19] in the study of sodium cobaltates.

3.1.2. Scaling and evidence for a single component. The extracted temperature dependence of the ^{57}Fe shift K_{ab} is presented in figure 2. Also shown are the ^{75}As (extended to high temperatures from a previous work [6]) and ^{139}La Knight shift in the ab-directions, K_{ab}, as measured in oriented $LaO_{0.9}F_{0.1}FeAs$ powder (2D powder) with a field $H_0 = 7.0494$ T applied along the ab-directions. The resonance frequencies of the central transitions of the As and La are given to second order by $f = \gamma H_0(1 + K_{ab}) + 3\nu_Q^2/16\gamma H_0$, with f being the frequency of

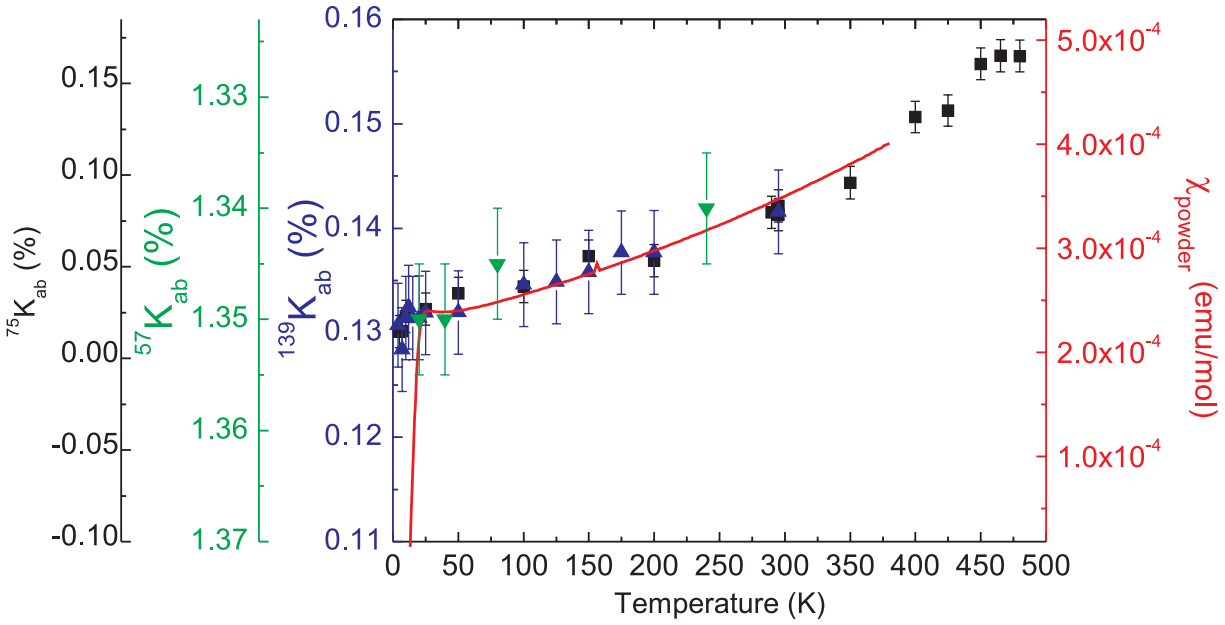

Figure 2. Knight shift of ^{75}As (black squares), ^{57}Fe (green down-pointing triangles) and ^{139}La (blue triangles), and the macroscopic susceptibility χ_{powder} (solid red line) versus temperature with different vertical scales and origins. Note the reversed scale for ^{57}Fe.

the peak of the 2D powder spectrum. For ^{75}As, we have independently measured $\nu_Q = 11.00(5)$ MHz (see figure 4 and [6]), and therefore we can extract K_{ab} from the spectrum. For the La, we measured the position of the satellites in a full spectrum, and found that $\nu_Q = 1.15(5)$ MHz. The macroscopic powder susceptibility measured in an applied field of 5 T is shown as a solid line. By proper scaling, the four data sets can be made to overlap in the paramagnetic region. The legitimacy of such a procedure is based on the fact that each shift can be written as the sum of a temperature-independent orbital shift K_{orb}, plus a spin shift K_s. Likewise, the static susceptibility can be written as the sum of a diamagnetic term χ_{dia} plus a Van Vleck-like term χ_{VV}, both expected to be temperature-independent, and a temperature-dependent spin term $\chi_{s,\text{macro}}$. Therefore the ratio of the scales of the NMR shifts to the scale of χ_{powder} reflects the strength of the hyperfine coupling of each nucleus to the spin susceptibility. It is remarkable that such a general scaling can be obtained, and suggests that the three nuclei probe the same component of spin susceptibility.

A priori this result is surprising, as there are several bands crossing the Fermi surface in the ferropnictides, and one might expect each band to supply a different contribution to the spin susceptibility with different hyperfine couplings to different bands. Such is the case for the oxygen in Sr_2RuO_4, which simultaneously couples to multiple bands with different temperature-dependent susceptibilities [20]. The Mila–Rice–Shastry picture in the cuprates, however, captures much of the relevant physics in terms of a single-spin component [21]–[24]. Our results suggest that if there are different hyperfine couplings to multiple orbitals in the ferropnictides, the spin response of each is nearly identical. This observation may reflect the itinerant rather than localized character of the Fe 3d electrons.

Table 2. Hyperfine couplings and orbital shifts for ^{139}La, ^{57}Fe and ^{75}As in the $LaO_{0.9}F_{0.1}FeAs$ compound. The results for ^{75}As are from the previous work [6].

	^{139}La	^{57}Fe	^{75}As
$A_{\rm hf}^{ab}$ (kOe/$\mu_{\rm B}$)	4.3(8)	−5.7(14)	25(3)
$K_{\rm orb}^{ab}$ (%)	0.12(1)	1.36(1)	−0.03(4)

The shift data in figure 2 clearly show a strong decrease of the spin susceptibility with a decrease in temperature, in agreement with several previous reports [5, 6, 8]. This suppression of low-energy spin excitations is similar to the behavior of the cuprates, and hence has been ascribed to the existence of a pseudogap in this system. In the cuprates, the spin susceptibility reaches a maximum at a temperature T^* that is doping-dependent. Since our Knight shift measurements indicate that susceptibility increases with an increase in temperature, we sought to find out whether this trend continues to higher temperature. Our ^{75}As measurements up to 480 K show no signature of a pseudogap peak, although the data hint at a leveling out by 500 K. It is unclear whether points at even higher temperatures could be gathered, as was for instance fruitful for $YBa_2Cu_4O_8$ [11], since SQUID measurements suggest a degradation of the sample. Note that the scaling of the NMR shift with $\chi_{\rm powder}$ remains good down to $T_{\rm c}$, which indicates the high quality of the samples, and the absence of any signature of a Curie contribution due to paramagnetic impurity spins, either intrinsic or belonging to a spurious phase.

3.1.3. Hyperfine couplings. Table 2 summarizes the hyperfine couplings and temperature-independent shifts extracted by plotting the measured shifts versus the bulk susceptibility as shown in figure 3, using equation (2). Since the anisotropic components of χ are unavailable in our aligned powder, we compare with the powder susceptibility in this determination, ignoring the modest anisotropy in temperature dependence between the c- and ab-directions [25]. We do not have an estimate for the non-spin component $\chi_{\rm VV} + \chi_{\rm dia}$ but it is between an overly cautious lower bound of 0 and an upper bound of roughly 2×10^{-4} emu mol^{-1}, otherwise the spin contribution would have to become negative below a certain temperature. This gives for the temperature-independent fraction of the shift $^{139}K_{\rm orb}^{ab} = 0.12(1)\%$ and $^{57}K_{\rm orb}^{ab} = 1.36(1)\%$.

The largest hyperfine coupling is to the As, which may be due in part to the fact that there are four nearest-neighbor iron atoms to each As. The fact that $^{139}A_{\rm hf}$ is roughly six times lower than $^{75}A_{\rm hf}$ is not surprising given that lanthanum is outside of the FeAs layers. In the case of iron, the negative hyperfine coupling suggests that the dominant hyperfine coupling is via a core polarization mechanism, but the small magnitude of the Fe hyperfine coupling is surprising. *A priori*, one would expect that iron would have the strongest coupling to the electronic properties, in light of theoretical predictions [26]–[28], indicating the highly predominant iron 3d character of the bands at the Fermi level. One explanation is that $^{57}A_{\rm hf} = A_{\rm cp} + A_{4\rm s}$, where $A_{\rm cp}$ (the core polarization contribution) is large and negative, whereas $A_{4\rm s}$ is large and positive, so the net coupling remains small.

From the measured lanthanum coupling, it is possible to estimate the value of the iron moment $m_{\rm Fe}$ in the magnetically frozen SDW state of the undoped LaOFeAs material. As there are no major structural changes between the 10% fluorine-doped material and the undoped material in its low-temperature state (aside from the slight orthorhombic distortion as a prelude to the magnetic transition), it is reasonable to assume that $^{139}A_{\rm hf}$ remains doping independent.

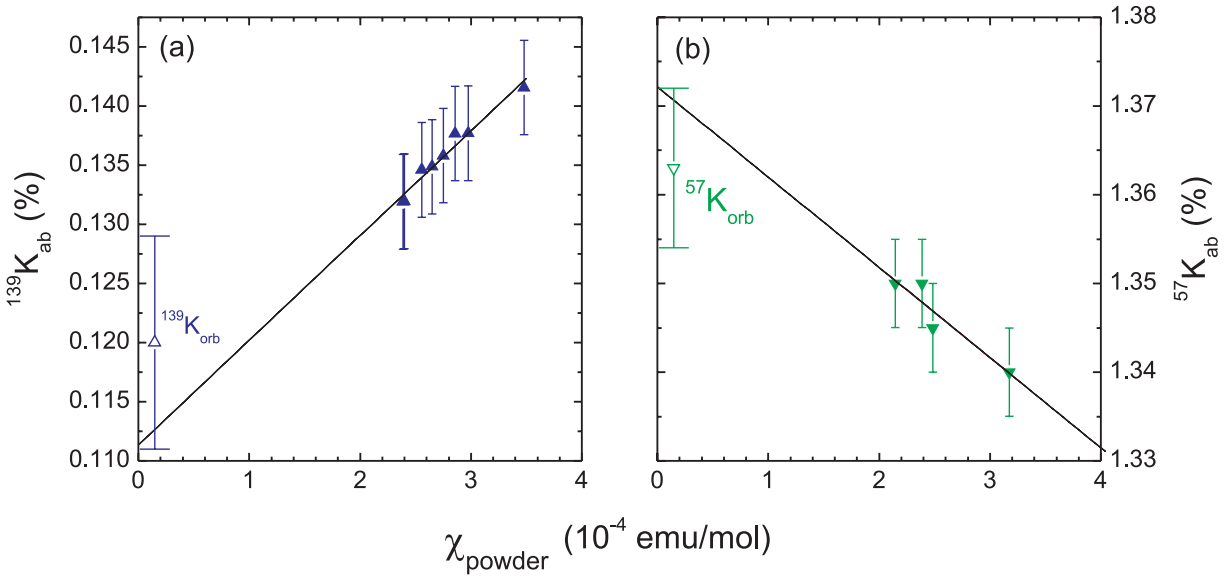

Figure 3. Knight shift of ^{139}La (a) and of ^{57}Fe (b) versus the macroscopic susceptibility χ_{powder}. The black lines are linear fits. The orbital shifts (see text) are shown next to the left vertical axes.

In this case, using the internal field of $H_{\text{int}}(\text{La}) = 2.5$ kOe measured by Nakai *et al* at the lanthanum site in the SDW state [7] and the relation $H_{\text{int}}(\text{La}) = {}^{139}A_{\text{hf}}\, m_{\text{Fe}}$, we estimate $m_{\text{Fe}} = 0.58(9)\mu_{\text{B}}$. While this is larger than the values obtained through the Mössbauer [10] and neutron scattering [9] measurements, which gave, respectively, $m_{\text{Fe}} = 0.25\mu_{\text{B}}$ and $m_{\text{Fe}} = 0.36\mu_{\text{B}}$, this result still points clearly at a largely itinerant situation in the SDW state.

3.2. Wavevector dependence of the susceptibility

As the superconductivity and frozen magnetism regions are close to each other in the phase diagram, it is natural to consider that spin fluctuations may play a role in the formation of Cooper pairs. NMR measurements of the spin lattice relaxation T_1^{-1} sample the low energy spin fluctuations via the dynamic susceptibility χ' [29]:

$$T_1^{-1} \propto \frac{\gamma_{\text{n}}^2 k_{\text{B}} T}{\gamma_{\text{e}}^2} \lim_{\omega \to 0} \sum_{\boldsymbol{q}} |A(\boldsymbol{q})|^2 \frac{\chi'_{\perp}(\boldsymbol{q}, \omega_0)}{\omega_0}, \tag{3}$$

where k_{B} is Boltzmann's constant, $\gamma_{\text{e/n}}$ the gyromagnetic ratios of the electron and the probed nucleus, ω_0 the Larmor frequency and $A(\boldsymbol{q})$ the hyperfine form factor of the probed nucleus. Particular attention should be paid to the $\boldsymbol{q}$-dependence of the latter, as filtering effects may occur such as in the superconducting cuprates [30], wherein the oxygens in the CuO_2 layers are not sensitive to antiferromagnetic fluctuations, whereas the copper nuclei are. Here, the fact that ^{57}Fe appears to be a particularly poor probe of the uniform ($\boldsymbol{q} = 0$) susceptibility compared with ^{75}As and ^{139}La, taking into account the crystallographic positions, suggests that hyperfine filtering effects might be at play. While the numerous superexchange paths make the analysis difficult for fluorine and lanthanum, Terasaki *et al* [18] show indeed that ${}^{75}A_{\text{hf}}(\boldsymbol{q})$ is well developed at $\boldsymbol{q} = 0$ and tends to vanish toward $\boldsymbol{q} = (\pi/a, \pi/a)$, whereas ${}^{57}A_{\text{hf}}(\boldsymbol{q})$ exhibits an opposite behavior, tending to low values about $\boldsymbol{q} = 0$.

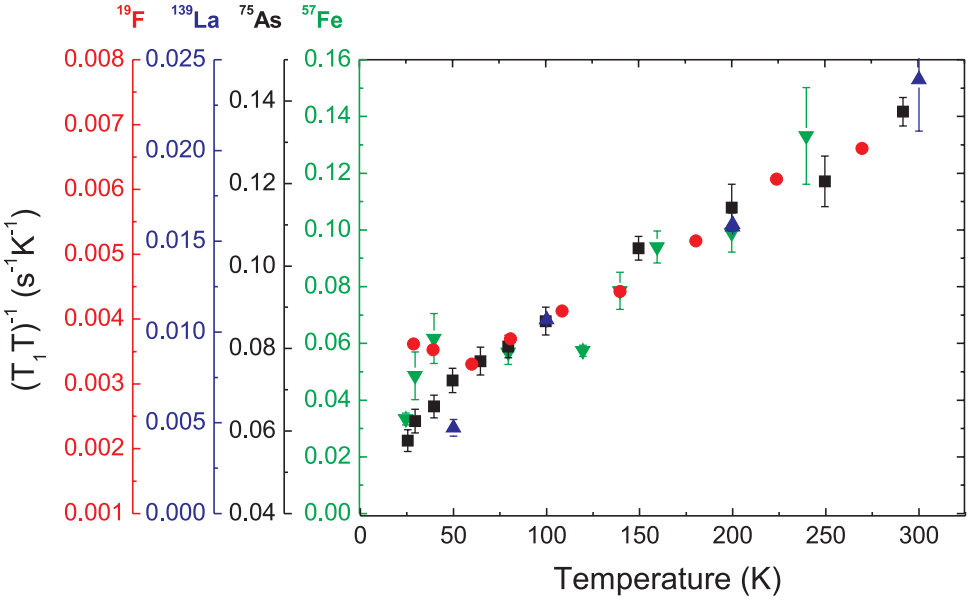

Figure 4. The temperature dependence of the ^{57}Fe, ^{75}As, ^{139}La and ^{19}F$(T_1T)^{-1}$. The ^{19}F data are reproduced from Ahilan *et al* [5]. For ^{139}La, ^{57}Fe and ^{75}As, T_1 along the ab-directions is used, while for fluorine it is $T_1^{\rm iso}$.

The temperature dependence of $(T_1T)^{-1}$ for each of the Fe, As and La nuclei is shown in figure 4, including ^{19}F data from Ahilan *et al* [5] for comparison. For ^{139}La, ^{57}Fe, and ^{75}As, T_1 along the ab-directions is used, whereas for fluorine it is $T_1^{\rm iso}$. The data are plotted with different axes, in order to highlight the similar temperature dependence for all four nuclei. The strength of the relaxation correlates with the distance to the iron plane, with the lowest values for the nuclei outside the FeAs planes. The spin lattice relaxation rate is largest for the Fe, whereas the spin shift at the Fe is relatively small compared with the other sites. In other words, $^{75}(T_1\,T\gamma_{\rm n}^2)/^{57}(T_1\,T\gamma_n^2) \approx 20$–$30$, whereas $(^{57}A_{\rm hf})^2(\boldsymbol{q}=0)/(^{75}A_{\rm hf})^2(\boldsymbol{q}=0) \approx 0.05$. There are two possible explanations for this discrepancy. Either there is a strong $\boldsymbol{q}$-space dependence of $\chi''(\boldsymbol{q},\omega)$, or there are multiple hyperfine coupling channels ($A_{\rm cp}$ and A_{4s}) between the Fe nuclear moments and the same degree(s) of spin freedom. Given the fact that the spin lattice relaxation rates for all the nuclei exhibit roughly the same temperature dependence as seen for the NMR shifts, any strong $\boldsymbol{q}$ dependence of the dynamic susceptibility seems unlikely. In other words, where the susceptibility is temperature dependent, the decrease occurs similarly across $\boldsymbol{q}$-space. Where some fluctuations in certain $\boldsymbol{q}$ regions cannot be ruled out in the absence of a refined analysis of hyperfine filtering effects, a simple explanation of our data would be that the relaxation comes mostly from quasi-particle scattering. In this case, the core polarization and the diamagnetic contributions to the Fe relaxation rate add up to the sum of the squares rather than a direct sum, as discussed in [31]. We note that there are no signatures of a pseudogap peak in the $(T_1T)^{-1}$ data, as observed in the cuprates [21, 32] in either the Fe or As data.

4. Spatial charge distribution

As a complementary study, we present in this section a theoretical analysis of the issue of the spatial charge distribution, based on our ^{75}As NQR measurements. The EFG observed at

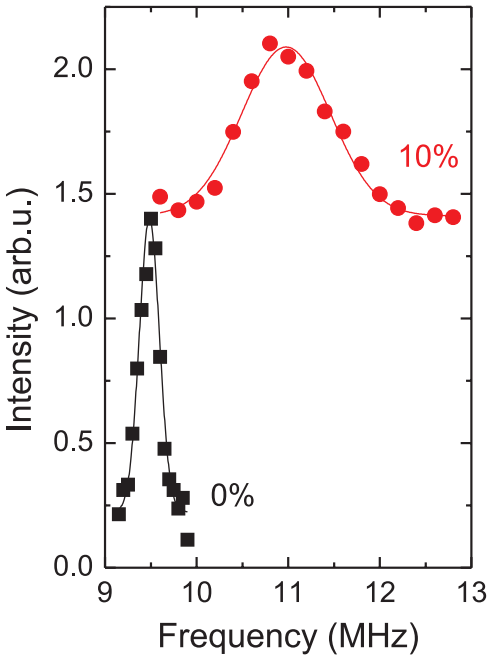

Figure 5. Room temperature ^{75}As NQR spectra in the doped $LaO_{0.9}F_{0.1}FeAs$ material and in the undoped parent compound LaOFeAs. Solid lines indicate Gaussian fits, with parameters given in the text.

the As site in the ferropnictides varies dramatically from one compound to the next, in stark contrast to the cuprates, where the EFGs are slightly doping dependent, but exhibit little variation among different families. To address this, we have measured the doping dependence of the NQR spectrum, and compared it with LDA calculations.

4.1. NQR results

In the ferropnictides, the ^{75}As nucleus quadrupolar moments interact with the EFG tensor giving rise to a resonance at the frequency

$$\nu_Q = \frac{3eQV_{zz}}{2I(2I-1)h}\sqrt{1+\eta^2/3}, \tag{4}$$

where η is the asymmetry of the EFG tensor. The EFG has the symmetry of the local atomic position, and depends on the local electronic density. We present in figure 5 the ^{75}As NQR spectrum at room temperature for the doped $LaO_{0.9}F_{0.1}FeAs$ material studied here, as well as for the undoped parent compound LaOFeAs. For both dopings, a well-defined line is observed, meaning that in each sample the EFG is the same at all As sites. This is in agreement with the single As crystallographic site and indicates spatially homogeneous doping. In the doped sample, the line is however significantly broader (full-width at half-maximum (FWHM) of 0.97(6) MHz) than in the undoped case (FWHM = 0.22(1) kHz). This could be explained by limited inhomogeneities of the fluorine concentration in the material, distributing somewhat the EFG, or even simply by the fact that As ions are at varying distances from the fluorine. We find that ν_Q increases from 9.48(1) MHz to 11.00(5) MHz on doping, which translates accordingly to a 16% increase of V_{zz}. This trend is in good agreement with measurements by Mukuda *et al* [33] on oxygen-deficient compounds.

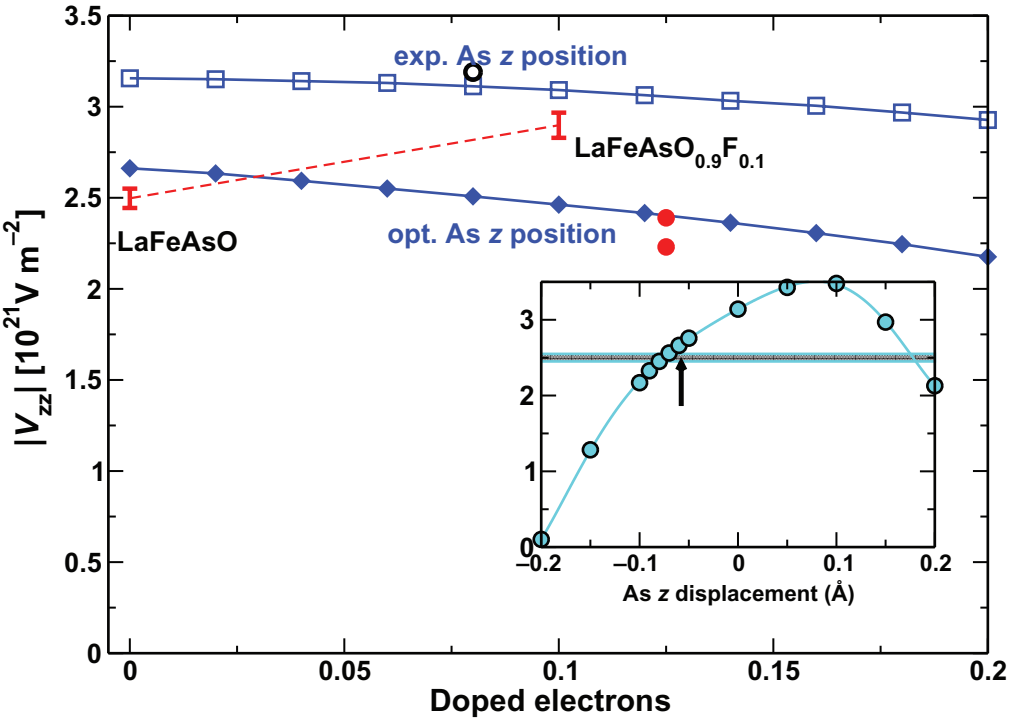

Figure 6. Calculated V_{zz} obtained from the virtual crystal approximation using the experimental As $z = 0.6507$ position (empty squares), the optimized As $z = 0.6438$ position (filled diamonds) and the $LaFeAsO_{0.92}F_{0.08}$ structure at 175 K (black circle). The red filled circles show the EFGs from the super cell calculation for the optimized As z position. The measured EFGs for the pure and the 10% F-doped compound are shown by error bars. Inset: dependence of ^{75}As V_{zz} on the As z position. The energetically optimized As z position is marked by an arrow. The experimental V_{zz} is represented by the shaded bar.

4.2. Comparison with theory

For the undoped compound the measured EFG is obtained by inserting the ^{75}As quadrupole moment [34] $Q = (3.14 \pm 0.06)$ b in equation (4), using $\eta = 0$, which yields $|V_{zz}^{\mathrm{exp}}| = (2.50 \pm 0.05) \times 10^{21}\,\mathrm{V\,m^{-2}}$. Using the 175 K lattice parameters and atomic positions as given in [9], we obtain fair agreement for the calculated EFG: $V_{zz}^{\mathrm{calc}} = -3.14 \times 10^{21}\,\mathrm{V\,m^{-2}}$. Like for the Fe magnetic moment, which in the calculations shows a strong dependence on the As z position [35, 36], we observe also for the EFG a strong As z dependence (inset of figure 6). The calculated EFG ($V_{zz}^{\mathrm{calc}} = -2.67 \times 10^{21}\,\mathrm{V\,m^{-2}}$) is much closer to the measured value when As is shifted along the negative z-direction to $z = 0.6438$, where the energy has a minimum (marked by an arrow in inset of figure 6) and the structure has a shorter Fe–As distance of 2.3748 Å.

The EFGs of the doped compounds were calculated with the virtual crystal approximation. The validity of the VCA was confirmed by super cell calculations. Due to the super cell construction, there are two different Wyckoff positions for As and hence two different EFGs, whereof one is lying on top of the VCA curve and the other one very close to it, see filled red circles in figure 6. First, we consider solely the effect of electron doping. Therefore, we

keep the structural parameters fixed for different levels of doping. In figure 6, two such VCA curves are shown. When the experimentally determined As $z = 0.6507$ position is used, the calculated and measured EFG values for 10% doping agree quite well. Also Lebègue *et al* [37] found good agreement for the 10% doped compound using the WIEN2k code. The VCA curve with the optimized As $z = 0.6515$ position is shifted in the direction of smaller $|V_{zz}|$. Now, we investigate the structural change on top of the doping by calculating the EFG within VCA for the 175 K data of $LaFeAsO_{0.92}F_{0.08}$ as given in [9]. This has only a minor effect on the EFG, as can be seen from the black circle in figure 6, which lies very close to the experimental VCA curve. We stress, at this point, that the effect of electron doping on the EFG is much smaller than the influence of the As z position as can be clearly seen by comparing figure 6 with the inset of figure 6.

Our calculations result in a decrease in $|V_{zz}|$ upon electron doping for $LaFeAsO_{0.9}F_{0.1}$, although in our experiments an increase is observed. This is not pointed out by Lebègue *et al* [37], although they obtain the same discrepancy for the trend in the V_{zz} calculation. Further studies are required to investigate the connection with intrinsic changes in the electronic structure.

For the NdFeAsO system, note that there is better agreement between the experimentally determined and the calculated EFG for the doped and for the undoped structure [38]. In that study, some of us (KK and HR) also showed that the 4f electrons have only a minor influence on the EFG, whereas the structure (chemical pressure) influences the EFG to a higher degree.

5. Conclusion

Using simultaneous ^{139}La, ^{57}Fe and ^{75}As NMR and NQR measurements, we have investigated the electronic properties of the $LaO_{1-x}F_xFeAs$ compound with $x = 0$ and 0.1. The ^{75}As NQR measurements show a sizable evolution of the EFG with doping that cannot be explained by LDA calculations, although the measured and calculated EFGs are in reasonable agreement for the undoped parent compound. Although a high sensitivity to the As z position is observed, the electronic origin of the difference from the experimental spectra remains unclear. The systematic scaling of the NMR shifts with the macroscopic susceptibility in the paramagnetic state suggests the presence of a single spin degree of freedom. Extending ^{75}As shift measurements up to 480 K reveals a continuous increase of the spin susceptibility with no sign of a peak, suggesting that the observed pseudogap behavior persists up to at least this high. We find that the hyperfine coupling to the iron is unexpectedly small, but speculate that there are, in fact, two components of the Fe hyperfine coupling with different signs. Consequently, the Knight shift at the Fe is rather small, but the spin lattice relaxation rate is large. Furthermore, we find that the spin lattice relaxation rates s for all four nuclei appear to scale with one another, providing further support for a single spin degree of freedom, and suggesting the absence of any significant structure in the dynamic susceptibility in $\boldsymbol{q}$-space. This result is surprising: in contrast with the cuprates, there appears to be very little spin fluctuation at low energies present in these superconducting samples. Detailed studies of the NMR relaxation and its doping dependence, as well as quantitative comparisons with inelastic neutron scattering data, should help bring further insights into the issue of the role of spin fluctuations in these materials. The origin of the strong temperature dependence of the susceptibility, as well as the presence of unconventional superconductivity in the absence of significant spin fluctuations, remain open questions, and indicate that physics of the iron pnictides is very different from that of the cuprates.

Acknowledgments

We thank M Deutschmann, S Müller-Litvanyi, R Müller, R Vogel and A Köhler for experimental support. This work was supported by the DFG, through FOR 538. DP acknowledges support from the DFG. GL acknowledges support from the Alexander von Humboldt-Stiftung.

References

[1] Kamihara Y, Watanabe T, Hirano M and Hosono H 2008 *J. Am. Chem. Soc.* **130** 3296
[2] Takahashi H, Igawa K, Arii K, Kamihara Y, Hirano M and Hosono H 2008 *Nature* **453** 376
[3] Yang J *et al* 2008 *Supercond. Sci. Technol.* **21** 082001
[4] Ren Z-A *et al* 2008 *Chin. Phys. Lett.* **25** 2215
[5] Ahilan K, Ning F L, Imai T, Sefat A S, Jin R, McGuire M A, Sales B C and Mandrus D 2008 *Phys. Rev.* B **78** 100501
[6] Grafe H-J *et al* 2008 *Phys. Rev. Lett.* **101** 047003
[7] Nakai Y, Ishida K, Kamihara Y, Hirano M and Hosono H 2008 *J. Phys. Soc. Japan* **77** 073701
[8] Klingeler R, Leps N, Hellmann I, Popa A, Hess C, Kondrat A, Hamann-Borrero J, Behr G, Kataev V and Buechner B 2008 arXiv:0808.0708v1
[9] de la Cruz C *et al* 2008 *Nature* **453** 899
[10] Klauss H-H *et al* 2008 *Phys. Rev. Lett.* **101** 077005
[11] Curro N J, Imai T, Slichter C P and Dabrowski B 1997 *Phys. Rev.* B **56** 877
[12] Kondrat A *et al* 2008 arXiv:0811.4436v1
[13] Luetkens H *et al* 2008 *Phys. Rev. Lett.* **101** 097009
[14] Koepernik K and Eschrig H 1999 *Phys. Rev.* B **59** 1743
[15] Perdew J P and Wang Y 1992 *Phys. Rev.* B **45** 13244
[16] Narita K, Umeda J and Kusumoto H 1966 *J. Chem. Phys.* **44** 2719
[17] Creel R B, Segel S L, Schoenberger R J, Barnes R G and Torgeson R D 1974 *J. Chem. Phys.* **60** 2310
[18] Terasaki N, Mukuda H, Yashima M, Kitaoka Y, Miyazawa K, Shirage P M, Kito H, Eisaki H and Iyo A 2009 *J. Phys. Soc. Japan* **78** 013701
[19] Mukhamedshin I R, Alloul H, Collin G and Blanchard N 2005 *Phys. Rev. Lett.* **94** 247602
[20] Imai T, Hunt A W, Thurber K R and Chou F C 1998 *Phys. Rev. Lett.* **81** 3006
[21] Takigawa M, Reyes A P, Hammel P C, Thompson J D, Heffner R H, Fisk Z and Ott K C 1991 *Phys. Rev.* B **43** 247
[22] Alloul H, Ohno T and Mendels P 1993 *Phys. Rev. Lett.* **63** 1700
[23] Mila F and Rice T M 1989 *Phys. Rev.* B **40** 11382–5
[24] Walstedt R E, Shastry B S and Cheong S-W 1994 *Phys. Rev. Lett.* **72** 3610–3
[25] Wang X F, Wu T, Wu G, Chen H, Xie Y L, Ying J J, Yan Y J, Liu R H and Chen X H 2008 arXiv:0806.2452v1
[26] Singh D J and Du M-H 2008 *Phys. Rev. Lett.* **100** 237003
[27] Ma F and Lu Z-Y 2008 *Phys. Rev.* B **78** 033111
[28] Vildosola V, Pourovskii L, Arita R, Biermann S and Georges A 2008 *Phys. Rev.* B **78** 064518
[29] Moriya T 1963 *J. Phys. Soc. Japan* **18** 516
[30] Mila F and Rice T M 1989 *Physica* C **157** 561
[31] Curro N J, Morales L, Soderholm L and Joyce J N M S D T J (ed) 2003 *Mat. Res. Soc. Symp.—Proc., Actinides—Basic Science, Applications and Technology* vol 802 pp 53–8
[32] Berthier C, Julien M H, Horvatić M and Berthier Y 1996 *J. Physique* I **6** 2205
[33] Mukuda H *et al* 2008 *J. Phys. Soc. Japan* **77** 093704
[34] Pyykkö P 2001 *Mol. Phys.* **99** 1617
[35] Krellner C, Caroca-Canales N, Jesche A, Rosner H, Ormeci A and Geibel C 2008 *Phys. Rev.* B **78** 100504
[36] Mazin I I, Johannes M D, Boeri L, Koepernik K and Singh D J 2008 *Phys. Rev.* B **78** 085104
[37] Lebègue S, Yin Z P and Pickett W E 2008 arXiv:0810.0376
[38] Jeglič P, Bos J-W G, Zorko A, Brunelli M, Koch K, Rosner H, Margadonna S and Arčon D 2009 unpublished